Hindawi
Oxidative Medicine and Cellular Longevity
Volume 2023, Article ID 5012474, 18 pages
https://doi.org/10.1155/2023/5012474

Research Article

The Interaction of Apelin and FGFR1 Ameliorated the Kidney Fibrosis through Suppression of TGFβ-Induced Endothelial-to-Mesenchymal Transition

Rongfen Gao,[1,2] **Yumin Wu**,[1] **Qian Yang**,[1] **Liangdong Chen**,[1] **Jiwei Chen**,[1] **Boyong Wang**,[1] **Zeming Liu**,[3] **Juan Jin**,[4] **Jinpeng Li**,[1] **and Gaosong Wu**[1]

[1]*Department of Thyroid and Breast Surgery, Zhongnan Hospital of Wuhan University, Wuhan 430000, China*
[2]*Department of Rheumatology and Immunology, Tongji Hospital, Tongji Medical College, Huazhong University of Science and Technology, Wuhan 430000, China*
[3]*Department of Plastic and Cosmetic Surgery, Tongji Hospital, Tongji Medical College, Huazhong University of Science and Technology, China*
[4]*Department of Nephrology, Zhejiang Provincial People's Hospital, Affiliated People's Hospital, Hangzhou Medical College, Hangzhou 310000, China*

Correspondence should be addressed to Zeming Liu; 6myt@tjh.tjmu.edu.cn, Juan Jin; lang_018@163.com, Jinpeng Li; lijinpeng3202@126.com, and Gaosong Wu; wugaosongtj@163.com

Received 14 February 2022; Revised 11 July 2022; Accepted 30 September 2022; Published 4 February 2023

Academic Editor: Alin Ciobica

Both epithelial-to-mesenchymal (EMT) and endothelial-to-mesenchymal (EndMT) transitions have shown to contribute to the development and progression of kidney fibrosis. It has been reported that apelin, a regulatory peptide, alleviates EMT by inhibiting the transforming growth factor β (TGFβ) pathway in renal diseases. Additionally, fibroblast growth factor receptor 1 (FGFR1) has been shown to be a key inhibitor of EndMT through suppression of the TGFβ/Smad pathway. In this study, we found that apelin and FGFR1 were spatially close to each other and that the apelin and FGFR1 complex displayed inhibitory effects on TGFβ/Smad signaling as well as associated EndMT in diabetic kidney fibrosis. In cultured human dermal microvascular endothelial cells (HMVECs), we found that the anti-EndMT and anti-TGFβ/Smad effects of apelin were dampened in FGFR1-deficient cells. Either siRNA- or an inhibitor-mediated deficiency of apelin induced the Smad3 phosphorylation and EndMT. Streptozotocin-induced CD-1 diabetic mice displayed EndMT and associated kidney fibrosis, which were restored by apelin treatment. The medium from apelin-deficient endothelial cells stimulated TGFβ/Smad-dependent EMT in cultured HK2 cells. In addition, depletion of apelin and the FGFR1 complex impaired CEBPA expression, and TGFβ-induced repression of CEBPA expression contributed to the initiation of EndMT in the endothelium. Collectively, these findings revealed that the interaction between apelin and FGFR1 displayed renoprotective potential through suppression of the TGFβ/Smad/CEBPA-mediated EndMT/EMT pathways.

1. Introduction

Kidney fibrosis represents the end-stage of all types of progressive chronic kidney disease (CKD). However, there is a lack of suitable strategies to reverse fibrosis in kidneys [1–3]. Previous studies have revealed that several mechanisms, including EMT and EndMT, are involved in the development and progression of renal fibrosis [4–6]. EMT is a biological repair process in which epithelial characteristics are lost, and mesenchymal markers are acquired. EndMT is a subtype of EMT in which endothelial cells lose characteristics such as smooth muscle α-actin (α-SMA), vimentin, and smooth muscle protein 22 α (SM22α) and gain mesenchymal characteristics such as VE-cadherin and CD31 (also known as platelet endothelial cell adhesion molecule-1) [7]. EMT and EndMT influence each other in the

diabetic kidney and accelerate fibrosis [8, 9]. EndMT is known to be associated with a variety of pathological changes, such as myocardial, pulmonary, and renal fibrosis, cancer proliferation and metastasis, and diabetic nephropathy [9–12]. Endothelial cells are stimulated by various cytokines, including transforming growth factor β (TGFβ), fibroblast growth factor (FGF), and interferon gamma (INF-γ) to undergo EndMT [11]. Overall, it has been shown that TGFβ is the main stimulant which induces EndMT through suppression of Smad3 activation [13–15].

Apelin is a regulatory peptide involved in various biological processes, including cardiovascular and fluid homeostasis, inflammation, cell proliferation, angiogenesis, and hepatic fibrosis [16, 17]. Apelin 13, identified as the major isoform [18], is a potent angiogenic regulator that activates the endothelial apelin receptor (APJ) [19, 20]. The apelin/APJ system is involved in the regulation of diabetes and diabetic complications such as diabetic kidney disease [16, 21–24]. Many medications have recently been found to improve EndMT and kidney fibrosis. For example, DPP-4, which interacts with integrinβ1, may lead to EndMT [25]. Furthermore, the DPP-4 inhibitor linagliptin inhibits EndMT and fibrosis [26]. Additionally, ACE inhibitors and the bioavailable peptide AcSDKP inhibit EndMT by inhibiting DPP-4 levels [27]. Previous studies have revealed that several mechanisms, including EMT and EndMT, are also involved in the development and progression of organ fibrosis [28–31]. Furthermore, emerging evidence demonstrates that apelin reduces EMT by targeting TGFβ in renal diseases [32, 33]. However, the molecular mechanisms underlying the effect of apelin on endothelial cells are poorly understood.

FGFR signaling plays a crucial role in various physiological processes, such as tissue and metabolism homeostasis, endocrine functions, and differentiation and EMT of their target cells [34, 35]. A previous study reported that apelin is related to aberrant expression of FGFR1 in the endothelial cells of the pulmonary arteries [36]. It was observed that apelin could attenuate renal fibrosis by suppressing the EMT of podocytes and tubules through TGFβ/Smad signaling [32, 33]. There is evidence that the inhibition of FGFR1 activates TGFβ signaling and induces EndMT [37–39]. Thus, it was assumed for the sake of this study that the interaction between apelin and FGFR1 suppresses TGFβ-induced EndMT in the progression of kidney fibrosis.

2. Materials and Methods

2.1. Reagents and Antibodies. The apelin peptide (ab152927) was purchased from Abcam (Cambridge, UK). The apelin inhibitor (ML221) (HY-103254) and recombinant human transforming growth factor β2 (HY-P7119) were purchased from MedChemExpress LLC (New Jersey, USA). Human neutralizing FGFR1 (MAB765) was obtained from R&D Systems (Minneapolis, MN, USA). Phosphor-Smad3-S423/S425 rabbit monoclonal antibody (AP0727) and vimentin rabbit monoclonal antibody (A19607) were obtained from ABclonal Technology (Wuhan, China). The following were obtained from Wuhan Sanying (Wuhan, China): E-cadherin rabbit polyclonal antibody (20874-1-AP), Smad3 rabbit polyclonal antibody (25494-1-AP), CEBPA polyclonal antibody (18311-1-AP), β-actin mouse monoclonal antibody (66009-1-lg), and GADPH rabbit monoclonal antibody (60004-1-lg). Mouse monoclonal anti-FGFR1 (ab824) and rabbit polyclonal anti-TGFβR2 (ab61213) antibodies were obtained from Abcam (Cambridge, UK). Rabbit anti-TGFβR1 (SAB4502958) antibody was purchased from Sigma-Aldrich (St. Louis, MO, USA). α-SMA rabbit monoclonal antibody was purchased from Cell Signaling Technology (Danvers, MA, USA). Rabbit polyclonal anti-SM22α antibody was obtained from Novus Biologicals (Littleton, CO, USA). Rabbit polyclonal anti-S100A4 (also known as FSP1) (PRB-497P), mouse monoclonal anti-VE-cadherin (sc-9989), and PECAM-1 (also known as CD31) (sc-365804) were purchased from Santa Cruz Biotechnology (Dallas, TX, USA).

2.2. Cell Culture and Treatment. The human dermal microvascular endothelial cells (HMVECs) were cultured in EBM-2 medium supplemented with EGM-2 which contained fetal bovine serum, 5.5 mmol/L-glucose, hydrocortisone, VEGF, R-IGF-1, hFGF-β, ascorbic acid, GA-1000, hEGF, and heparin (Lonza, Alpharetta, GA, USA). When the cells reached 70-80% confluence, TGFβ2 (5 ng/mL), N-FGFR1 (1.5 μg/mL), apelin (100 nM), or ML221 (10 μM) was added to the experimental medium (a mixture of HuMedia-MVG in serum-free RPMI 1640 medium at a 1 : 3 ratio).

Human HK-2 cells were cultured in MEM supplemented with 10% fetal bovine serum (Invitrogen, Carlsbad, CA, USA). To establish the conditioned medium experiment [8], HMVECs were transfected with scramble or apelin siRNA for 6 h, after which the medium was replaced with fresh EBM-2 medium. After incubation with fresh medium for 48 h, the experimental medium of HMVECs was harvested and transferred to cultured HK2 cells.

2.3. Transfection Experiments. HMVECs were transfected with siRNA (100 nmol/L) targeting apelin and CEBPA. The apelin siRNA sequences were 5′-GCAUCCCAAAUCGG UUCUATT-3′ and 3′-UAGAACCGAUUUGGGAUGCTT-5′. The CEBPA siRNA sequence was 5′-CCUUCAACGAC GAGUUCCUTT-3′ and 3′-AGGAACUCGUCGUGAAGGT T-5′. For transient transfection of siRNAs, cells at ~60% confluence were transfected with Lipofectamine RNAiMAX (13778100, Invitrogen).

2.4. Duolink In Situ Assay. The manufacturer's protocol for the Duolink *in situ* proximity ligation assay (PLA) was followed. HMVECs were cultured with TGFβ2 (5 ng/mL) or N-FGFR1 (1.5 μg/mL) for 48 h with and without apelin preincubation. After fixing with 4% paraformaldehyde, cells were permeabilized with 0.2% Triton X-100. After blocking, the cells were treated with rabbit antiapelin and mouse anti-FGFR1 antibodies overnight. The cells were incubated for 1 h at 37°C with the PLA probe solution before being treated with ligase solution for 30 min at 37°C and a polymerase amplification solution for 100 min at 37°C. The samples were promptly mounted for 20 min with Duolink *in situ*

mounting medium containing DAPI, and fluorescence microscopy was used for the examination. The images were evaluated from six separate view fields at ×400 magnification for each slide.

2.5. Western Blot Analysis. RIPA lysis buffer (ABclonal Technology Co., Wuhan, China) was used to lyse nuclear and cytoplasmic proteins. Protein lysates were boiled for 10 min at 100°C in SDS sample buffer and transferred to PVDF membranes after separation on SDS-polyacrylamide gels. Next, 5% skim milk was used to block the mixture. After blocking, the membranes were incubated overnight at 4°C with primary antibodies, followed by incubation with secondary antibodies for 1 h at room temperature. Blots were analyzed using a chemiluminescence imaging system (Tanon, Shanghai, China).

2.6. Immunofluorescence for Cell Culture. The treated HMVECs were plated on six-well culture slides (354630, BioCoat) for 48 h. 100% methanol was used to fix the cells for 10 min at -20°C, which was followed by acetone for 1 min at -20°C. After that, the cells were blocked with 2% bovine serum albumin (BSA) for 30 min at room temperature and then incubated with the primary antibody, followed by binding to the corresponding secondary antibodies for 30 min. Finally, PBS was used to thoroughly wash the mixture three times, and a mounting medium containing DAPI was used to mount it. A fluorescence microscope (Axio Vert. A1, Carl Zeiss Microscopy GmbH) was used to visualize all images.

2.7. Immunostaining Analysis of Mouse Tissues. Briefly, acetone was used to fix the frozen kidney sections for 10 min at -20°C. The sections were blocked with 2% BSA for 30 min at room temperature, followed by incubation with primary antibodies against CD31/FSP1, CD31/α-SMA, and CD31/vimentin. The corresponding secondary antibodies were used to incubate the sections successively. The mounting medium containing DAPI was then mounted for 10 min at room temperature. A fluorescence microscope (Axio Vert. A1, Carl Zeiss Microscopy GmbH) was used to visualize all images.

2.8. Morphological Evaluation. PAS-stained glomeruli from each mouse were detected using a digital microscope screen grid containing 540 (27×20) points. Based on Masson's trichrome-stained and Sirius red-stained tissue images of each section, fibrotic areas were evaluated. Six separate fields from each mouse were analyzed at ×40 magnification.

2.9. Animal Experiments. Male CD-1 mice (4 weeks old) were obtained from Beijing Vital River Laboratory Animal Technology Co., Ltd. (Beijing, China) and randomly divided into control, STZ-treated CD-1, and apelin-treated STZ mice, according to a previous study [38, 40]. Briefly, 8-week-old CD-1 mice were intraperitoneally injected with streptozotocin (STZ; 200 mg/kg). Sixteen weeks after the induction of diabetes, the STZ-treated mice were assigned to the nontreatment group or the apelin treatment group (500 μg/kg BW/day using an osmotic minipump for 8 weeks). Animal experiments were performed in the laboratory animal facility of Zhongnan Hospital of Wuhan University according to the requirements of animal ethics and were approved by the Laboratory Animal Management and Use Committee of the Animal Experiment Center of Wuhan University (WP2020-08103).

2.10. Statistical Analysis. Statistical analyses were conducted using GraphPad Prism software (version 8.0). Data are expressed as mean ± SD of at least three independent experiments. Two group comparisons were performed using an unpaired two-tailed t -test (statistical significance was defined as $P < 0.05$). Ns indicates nonsignificant ($^{*}p < 0.05$, $^{**}p < 0.01$, $^{***}p < 0.001$, and $^{****}p < 0.0001$).

3. Results

3.1. Proximity of Apelin and FGFR1 for the Suppression of TGFβ/Smad Signaling Pathway in the Endothelium. To examine the proximity between apelin and FGFR1 in cultured HMVECs, we performed Duolink *in situ* PLA. The results showed close proximity between apelin and FGFR1 in normal cultured HMVECs, indicating that endogenous apelin interacts with FGFR1 (Figure 1(a)). In the presence of a neutralizing FGFR1 antibody (N-FGFR1), the close proximity between apelin and FGFR1 was diminished in endothelial cells (Figure 1(a)). However, proximity was not restored by exogenous apelin incubation in the presence of N-FGFR1, suggesting that FGFR1 is a downstream target of apelin (Figure 1(a)). Western blot analysis showed that endogenous apelin restored TGFβ2 and suppressed FGFR1 expression in HMVECs, indicating the inhibitory effect of TGFβ2 on the apelin and FGFR1 complex (Figures 1(b) and 1(c)).

We then investigated whether exogenous apelin could suppress the TGFβ/Smad signaling pathway in the endothelium. In the presence of TGFβ2, the close proximity between apelin and FGFR1 was significantly diminished, and exogenous apelin incubation reversed this proximity, suggesting that TGFβ2 inhibited the interaction between apelin and FGFR1 (Figure 1(a)). Apelin significantly inhibited TGFβ2-induced Smad3 phosphorylation (p-smad3), TGFβR1, and TGFβR2 levels, which confirmed the inhibitory effect of apelin on TGFβ/Smad signaling (Figure 1(b)). Additionally, exogenous apelin treatment significantly promoted the expression of FGFR1 in the endothelium (Figure 1(c)).

3.2. Apelin Inhibits TGFβ/Smad Signaling and EndMT via Regulating FGFR1 Expression in Endothelial Cells. To further study the role of apelin in the regulation of TGFβ-induced EndMT, western blotting was performed to detect protein levels of Smad3, p-Smad3, FGFR1, and EndMT markers. Exogenous apelin treatment significantly increased CD31 and VE-cadherin levels and decreased SM22α, FSP1, and α-SMA levels in cultured HMVECs. In addition, TGFβ2-induced EndMT was reversed by exogenous apelin treatment, which verified that apelin suppressed TGFβ-induced EndMT (Figure 2(a)).

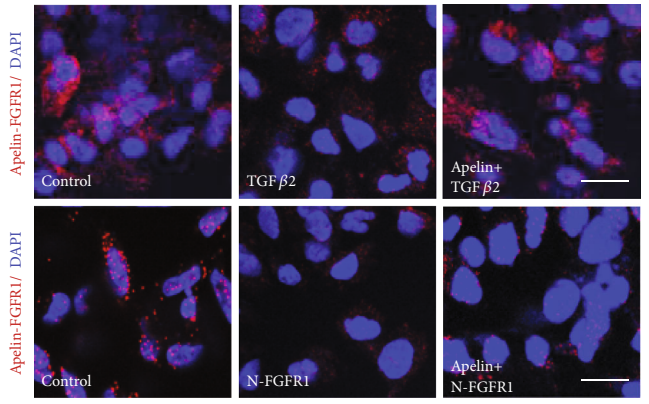

(a)

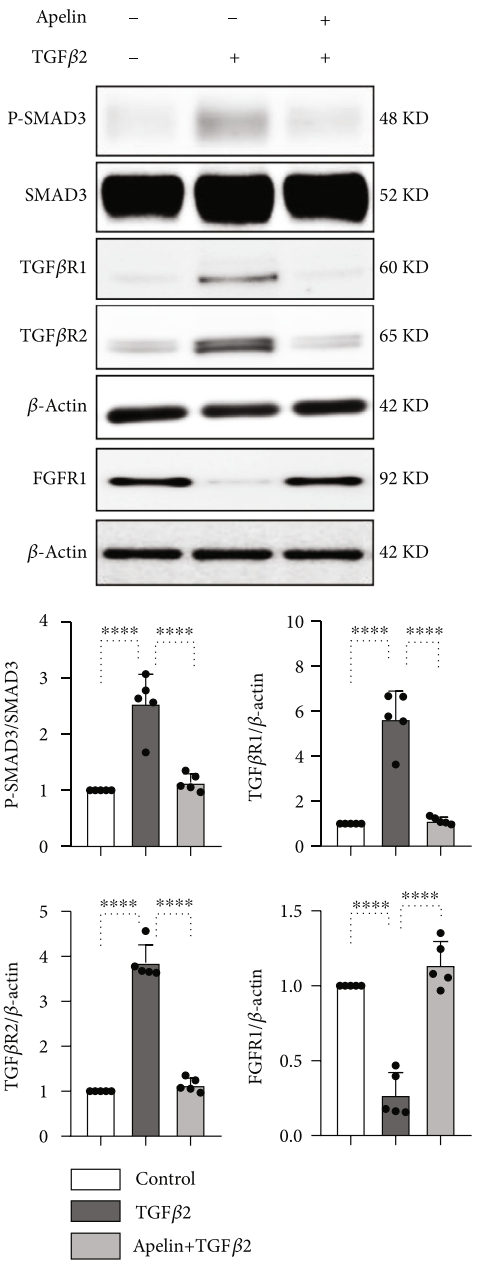

(b)

Figure 1: Continued.

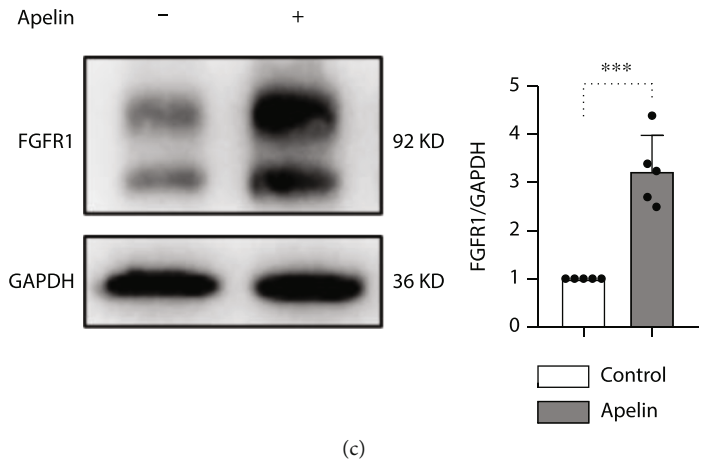

(c)

Figure 1: Proximity between apelin and FGFR1 suppresses the TGFβ/Smad signaling pathway in HMVECs. (a) HMVECs were treated with TGFβ2 (5 ng/mL) or N-FGFR1 (1.5 μg/mL) for 48 h with or without preincubation with apelin (100 nM) for 2 h. The proximity between apelin and FGFR1 was then analyzed by the Duolink In Situ Assay. For each slide, images at a ×400 original magnification were obtained from six different areas. The scale bar is 60 μm in each panel. (b) HMVECs were treated with TGFβ2 (5 ng/mL) or with apelin (100 nM) for 48 h, and the p-Smad3, TGFβR1, TGFβR2, and FGFR1 levels were analyzed by western blot. Densitometric analysis of the p-Smad3/Smad3, TGFβR1/β-actin, TGFβR2/β-actin, and FGFR1/β-actin levels from each group ($n = 5$) was analyzed. (c) HMVECs were treated with or without apelin (100 nM) for 48 h, and the FGFR1 levels were analyzed by western blot. Densitometric analysis of the FGFR1/GADPH levels from each group ($n = 5$) was analyzed.

Previous studies have confirmed that the inhibition of FGFR1 activates TGFβ/Smad signaling and induces EndMT [6, 37]. We then investigated whether apelin inhibited TGFβ/Smad signaling and EndMT by regulating FGFR1 expression. N-FGFR1 treatment significantly increased p-Smad3 expression and EndMT in endothelial cells, and apelin could not reverse N-FGFR1-induced Smad3 activation and EndMT, suggesting that the anti-EndMT and anti-TGFβ/Smad effects of apelin were lost in FGFR1-deficient cells (Figure 2(b)).

TGFβ2 has been shown to be a strong activator of Smad3 and downstream EndMT [37], and endothelial apelin knockdown showed a consistent effect. siRNA-mediated knockdown of apelin increased p-Smad3 expression and EndMT in endothelial cells, especially when TGFβ2 and apelin siRNAs were applied together (Figure 2(c)). An apelin inhibitor (ML221) also showed a similar result, suggesting that inhibition of apelin downregulated FGFR1 and promoted TGFβ-induced EndMT (Figure 2(d)).

3.3. Conditioned Medium from Apelin-Knockdown HUVECs Mediates the Induction of EMT in HK2 Cells. To address whether apelin deficiency in the endothelium could influence the extent of EMT in renal tubular cells, we established a conditioned medium experiment to test whether apelin knockdown could enhance EMT in HK2 cells, an immortalized human proximal tubule epithelial cell line (Figure 3(a)). The experimental medium from apelin siRNA-transfected HUVECs, but not that from scramble siRNA-transfected HUVECs, significantly decreased E-cadherin levels and increased vimentin and α-SMA levels in HK-2 cells, indicating that apelin knockdown in endothelial cells induced EMT in tubular epithelial cells (Figure 3(b)). We also measured TGFβ1 levels in the medium of apelin or scramble siRNA-transfected HUVECs, and apelin knockdown remarkably increased TGFβ1 levels compared to those in the control group (Figure 3(c)).

3.4. CEBPA Knockdown Promotes TGFβ-Mediated EndMT. It has been reported that CEBPA (C/EBPα) is a Smad3-repressed target during TGFβ-induced EMT in human breast cancer [41, 42]. To further evaluate the effect of CEBPA on endothelial cells, western blotting and immunofluorescence were performed to detect the expression of EndMT markers. Knockdown of CEBPA significantly decreased VE-cadherin levels and increased the expression of α-SMA, vimentin, SM22α, and exogenous TGFβ2, and/or apelin did not influence the expression levels of EndMT markers (Figures 4(a) and 4(b)). In addition, CEBPA expression was inhibited in the presence of TGFβ2, whereas exogenous apelin treatment significantly increased CEBPA expression. When TGFβ2 and apelin were applied together, the CEBPA expression level was slightly increased compared to that in the control group (Figure 4(c)). To verify the interaction between apelin, the FGFR1 complex, and CEBPA, HUVECs were treated with N-FGFR1 and apelin. CEBPA was significantly suppressed in the presence of N-FGFR1, and apelin restored the inhibitory effect of FGFR1 deficiency (Figure 4(d)). Immunofluorescence analysis also showed that the loss of CEBPA induced EndMT in the endothelium, and the expression of CD31, VE-cadherin, and α-SMA was not affected by exogenous TGFβ2 and/or apelin treatment, indicating that CEBPA is a downstream target of apelin/TGFβ signaling (Figures 4(e) and 4(f)).Taken together, these results strongly indicate that depletion of apelin and the FGFR1 complex could impair CEBPA expression, and the

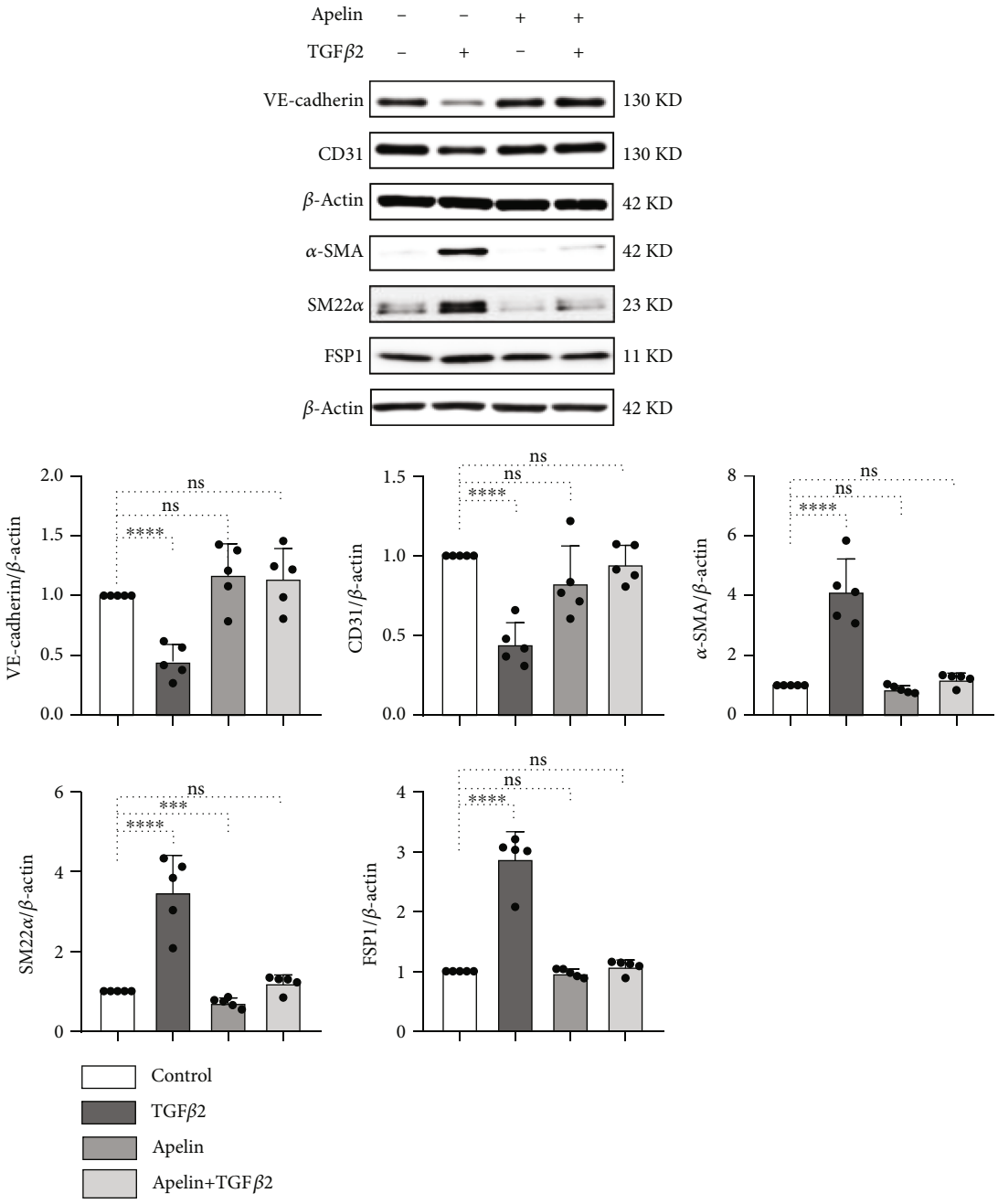

(a)

Figure 2: Continued.

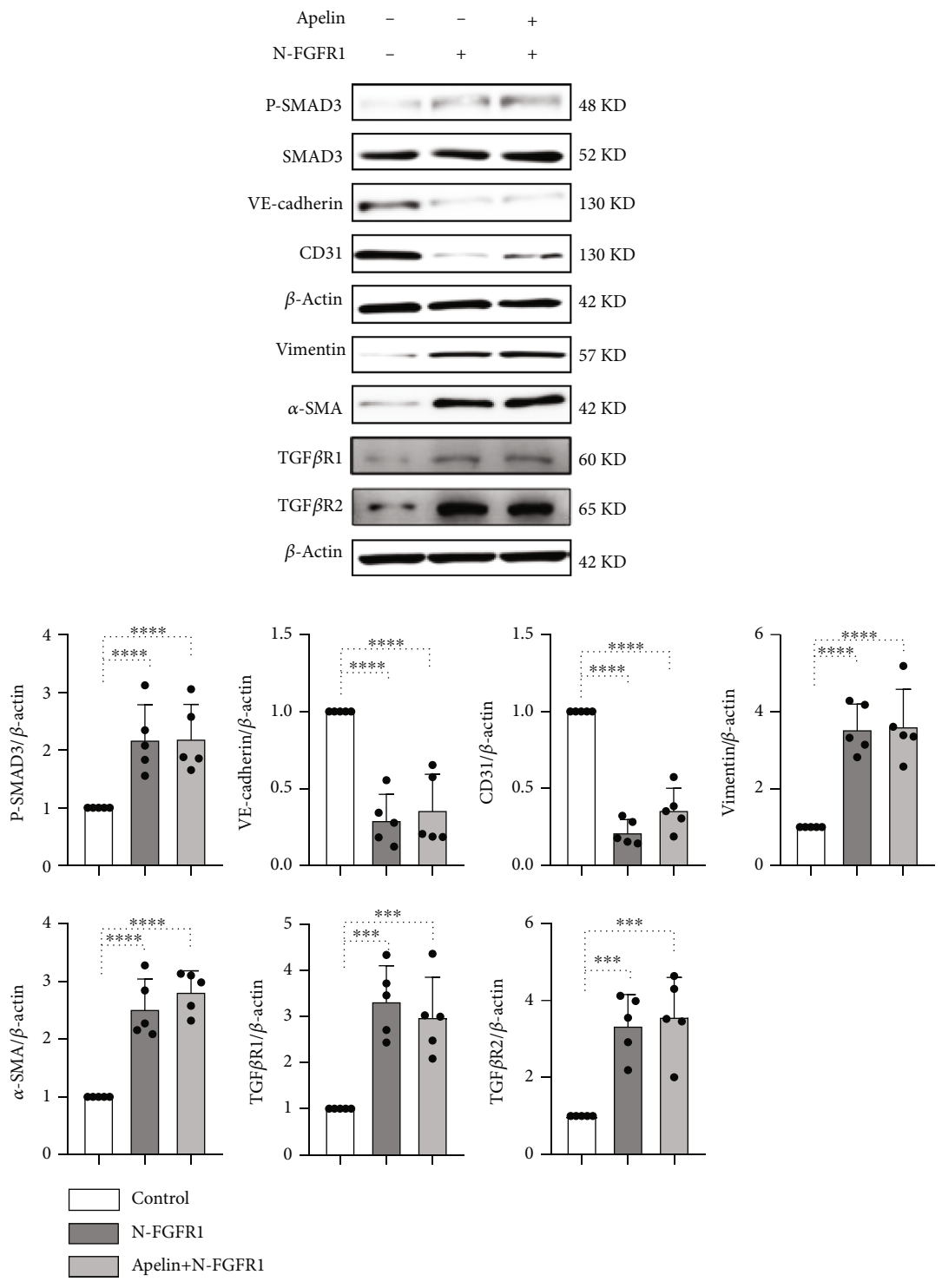

(b)

Figure 2: Continued.

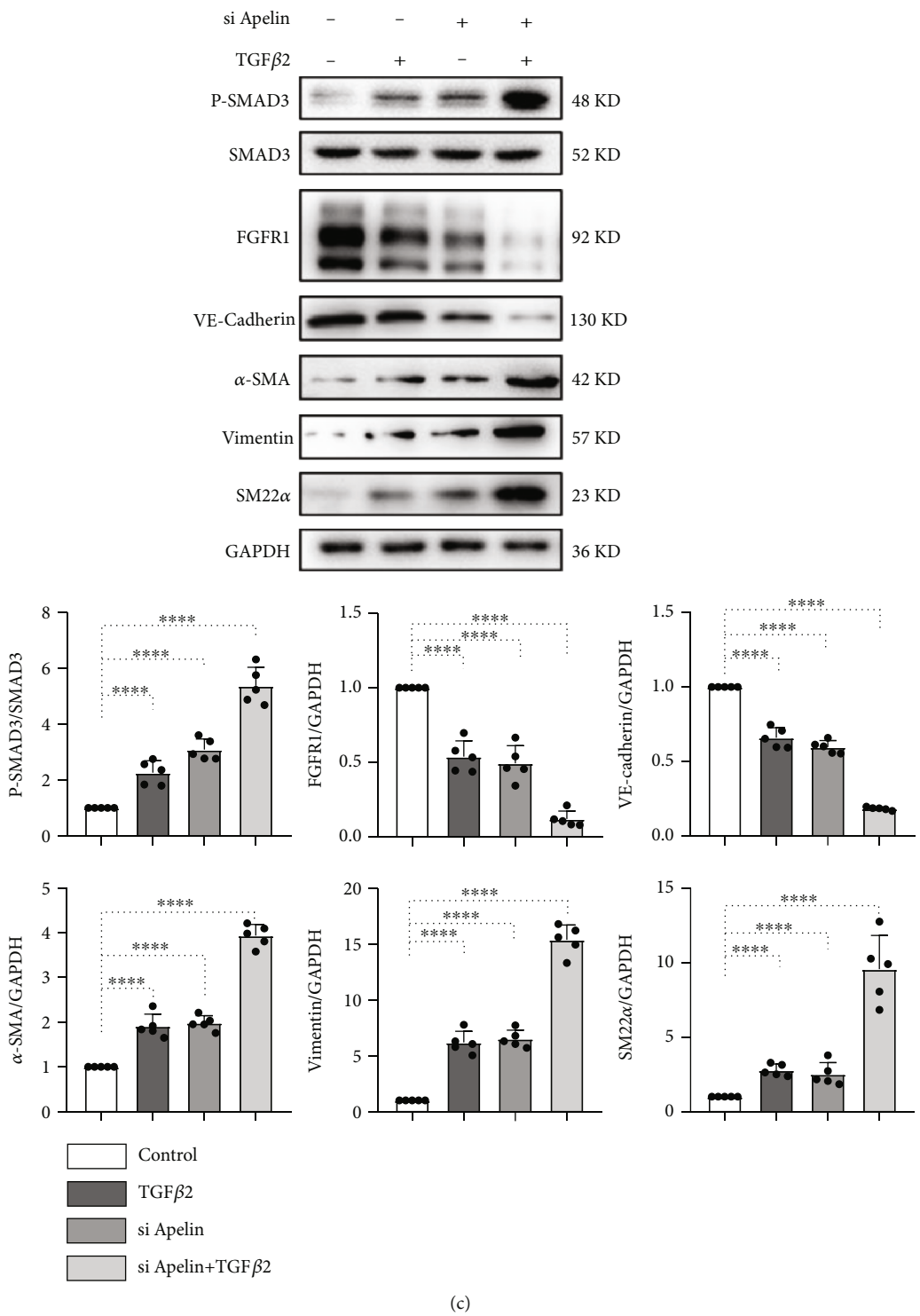

(c)

Figure 2: Continued.

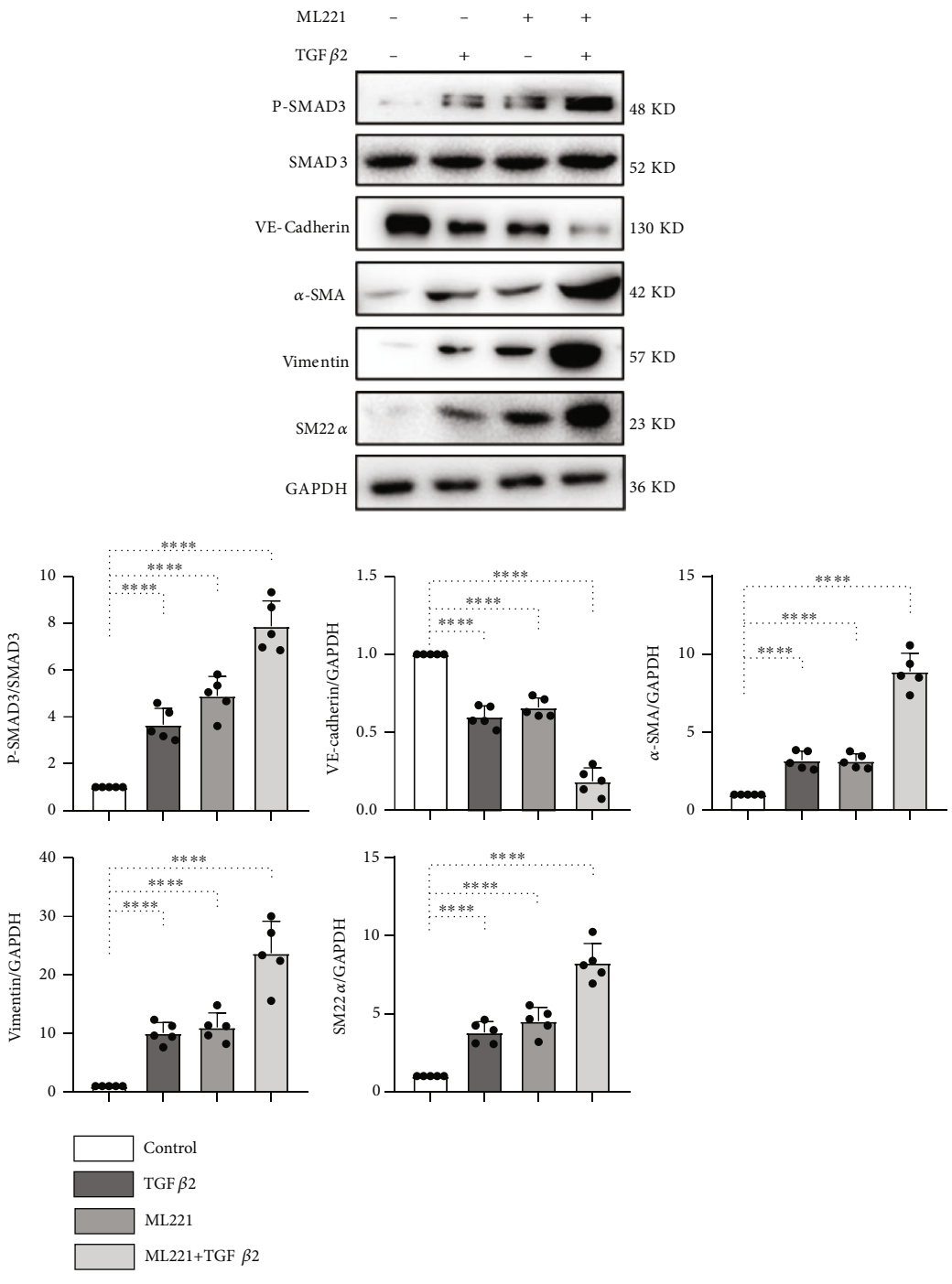

(d)

Figure 2: Apelin inhibits TGFβ/Smad signaling and EndMT via regulating FGFR1 expression. (a) HMVECs were treated with TGFβ2 (5 ng/mL) for 15 min or 48 h with or without preincubation with apelin for 2 h, and the VE-cadherin, CD31, α-SMA, SM22α, and FSP1 levels were analyzed by western blot. Densitometric analysis of the VE-cadherin/β-actin, CD31/β-actin, α-SMA/β-actin, SM22α/β-actin, and FSP1/β-actin levels from each group ($n = 5$) was analyzed. (b) HMVECs were incubated with N-FGFR1 (1.5 μg/mL) in the presence or absence of apelin for 48 h, and the p-Smad3, VE-cadherin, CD31, vimentin, and α-SMA levels were analyzed by western blot. Densitometric analysis of the p-Smad3/Smad3, VE-cadherin/β-actin, CD31/β-actin, vimentin/β-actin, and α-SMA/β-actin levels from each group ($n = 5$) was analyzed. (c) HMVECs were transfected with or without apelin siRNA for 48 h in the presence or absence of TGFβ2, and the p-smad3, FGFR1, VE-cadherin, α-SMA, vimentin, and SM22α levels were analyzed by western blot. Densitometric analysis of the p-Smad3/Smad3, FGFR1/GADPH, VE-cadherin/GADPH, α-SMA/GADPH, vimentin/GADPH, and SM22α/GADPH levels from each group ($n = 5$) was analyzed. (d) HMVECs were incubated with or without ML221 (apelin inhibitor, 10 μM) for 48 h in the presence or absence of TGFβ2, and the p-smad3, VE-cadherin, α-SMA, vimentin, and SM22α levels were analyzed by western blot. Densitometric analysis of the p-Smad3/Smad3, VE-cadherin/GADPH, α-SMA/GADPH, vimentin/GADPH, and SM22α/GADPH levels from each group ($n = 5$) was analyzed.

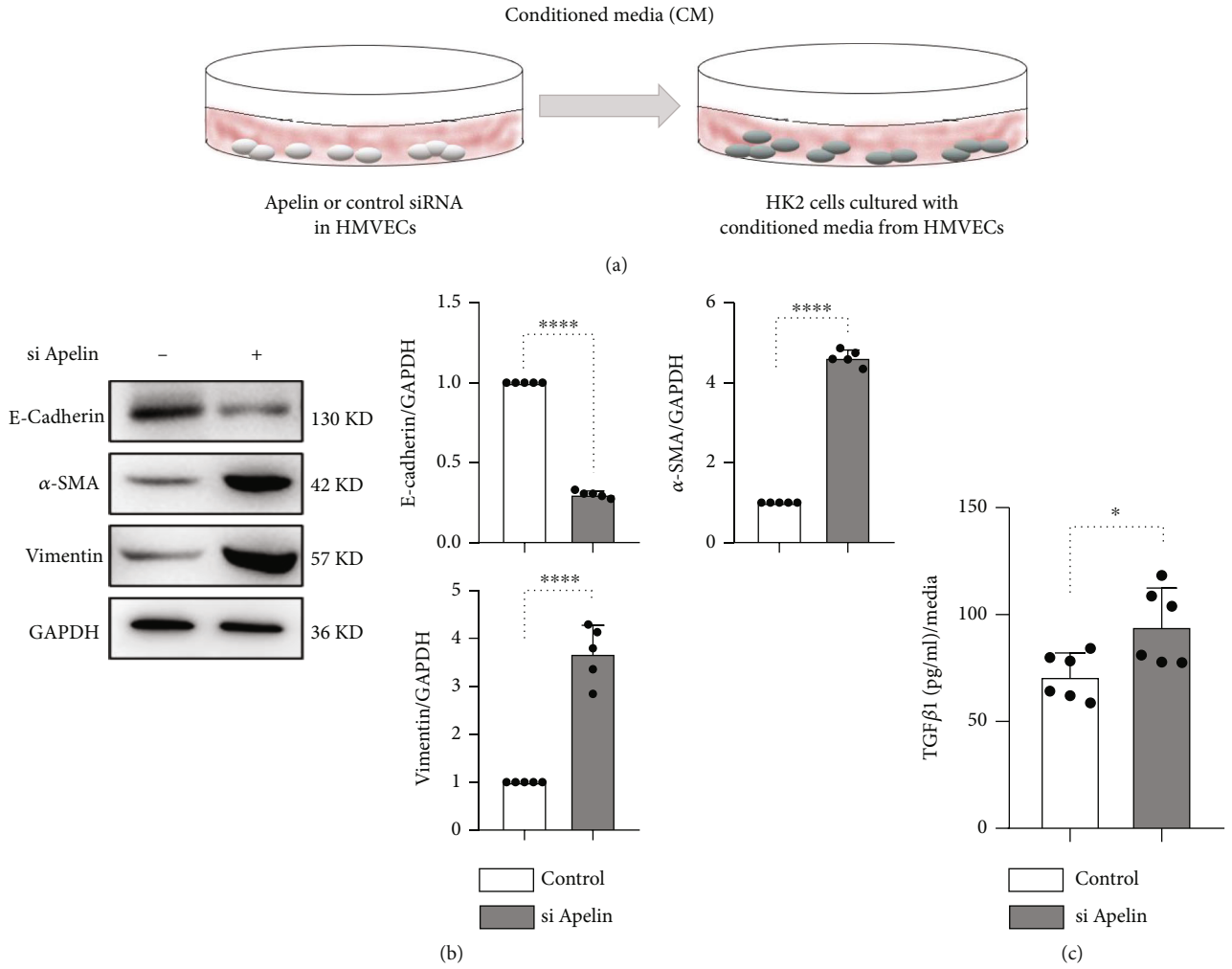

Figure 3: Apelin deficiency stimulates neighboring epithelial cells to transition into mesenchymal cells. (a) Design of the conditional medium experiment. HUVECs were transfected with scramble or apelin siRNA, and after 6 h, the medium was replaced with fresh medium and incubated for 48 h. After incubation of fresh medium for 48 h, the experimental media of HUVECs were harvested and transferred to cultured HK2 cells. (b) HK2 cells incubated with conditioned medium from apelin-knockdown HMVECs for 48 h, and the E-cadherin, vimentin, and α-SMA levels were analyzed by western blot. Densitometric analysis of the E-cadherin/GADPH, α-SMA/GADPH, and vimentin/GADPH levels from each group ($n = 5$) was analyzed. (c) ELISA analysis of TGFβ1 levels from conditioned medium.

TGFβ-induced repression of CEBPA expression contributed to the initiation of EndMT.

3.5. Apelin Inhibits Diabetes-Induced EndMT In Vivo. To identify the anti-EndMT and antifibrosis effect of apelin in vivo, we established the apelin-treated streptozotocin-(STZ-) induced diabetic mouse model. Masson's trichrome staining (MTS) results showed that the collagen fibers, stained blue, were significantly increased in diabetic kidney, suggesting massive organ fibrosis in diabetic mice (Figures 5(a) and 5(b)). However, the kidney and heart tissues of apelin-treated diabetic mice showed minor fibrotic alterations (Figures 5(c) and 5(d)). The similar phenomenon was observed in heart tissues that fibrotic alterations were ameliorated with the treatment of apelin in diabetic mice (Figures 5(e)–5(h)). In the kidneys, Sirius red staining demonstrated that the red-colored collagen was markedly increased, consistent with the MTS results (Figures 5(i)–5(l)). Periodic acid-Schiff (PAS) staining was used to evaluate the glomerular structure and damage in diabetic kidneys. The results showed that apelin inhibited ECM deposition, collagen accumulation, and glomerulosclerosis in the kidneys of apelin-treated diabetic mice (Figures 5(m)–5(p)).

In addition, we analyzed endothelial cells in the kidneys undergoing EndMT by co-immunolabeling of FSP1 and α-SMA with CD31. Compared with the control group, diabetic kidneys showed more endothelial cells undergoing EndMT, suggesting that apelin remarkably suppressed diabetes-induced endothelial damage (Figure 6). Moreover, the mRNA level of other fibrosis markers and other TGF beta signaling molecules was not remarkably influenced by the treatment of apelin, like fibronectin, collagen-1, collagen

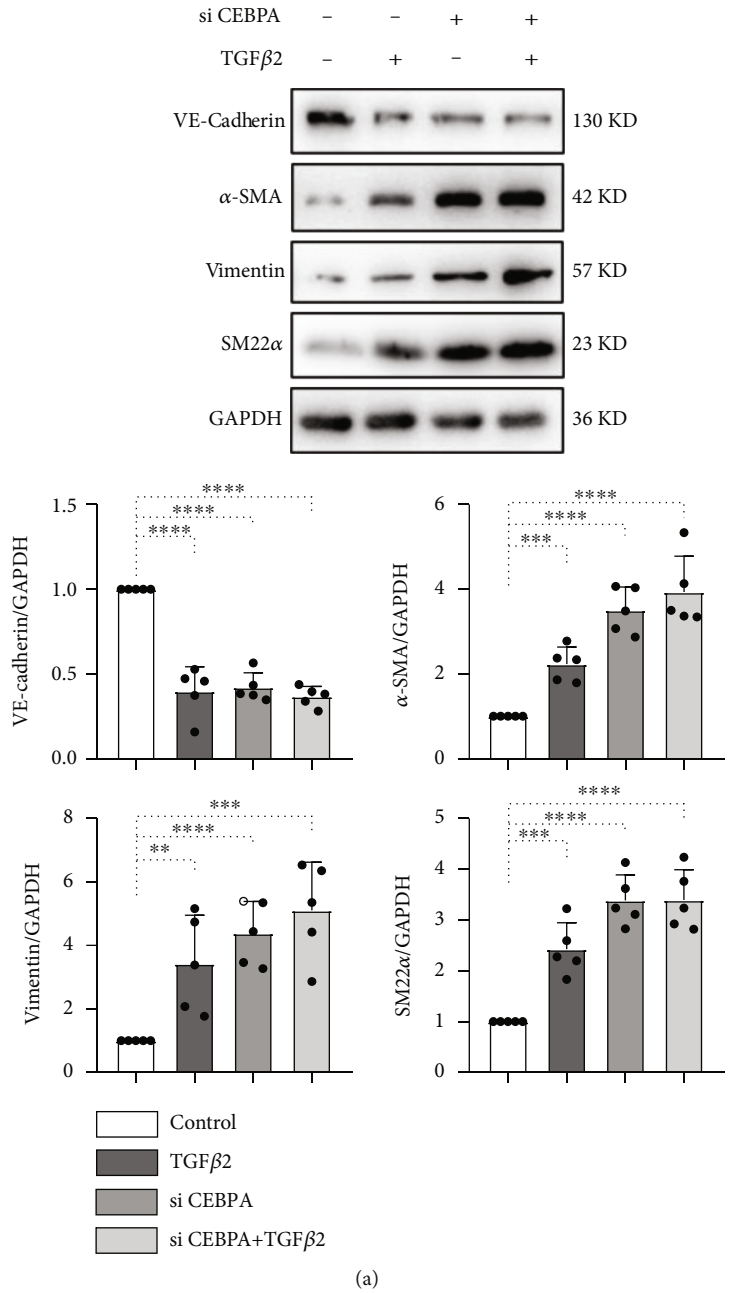

(a)

Figure 4: Continued.

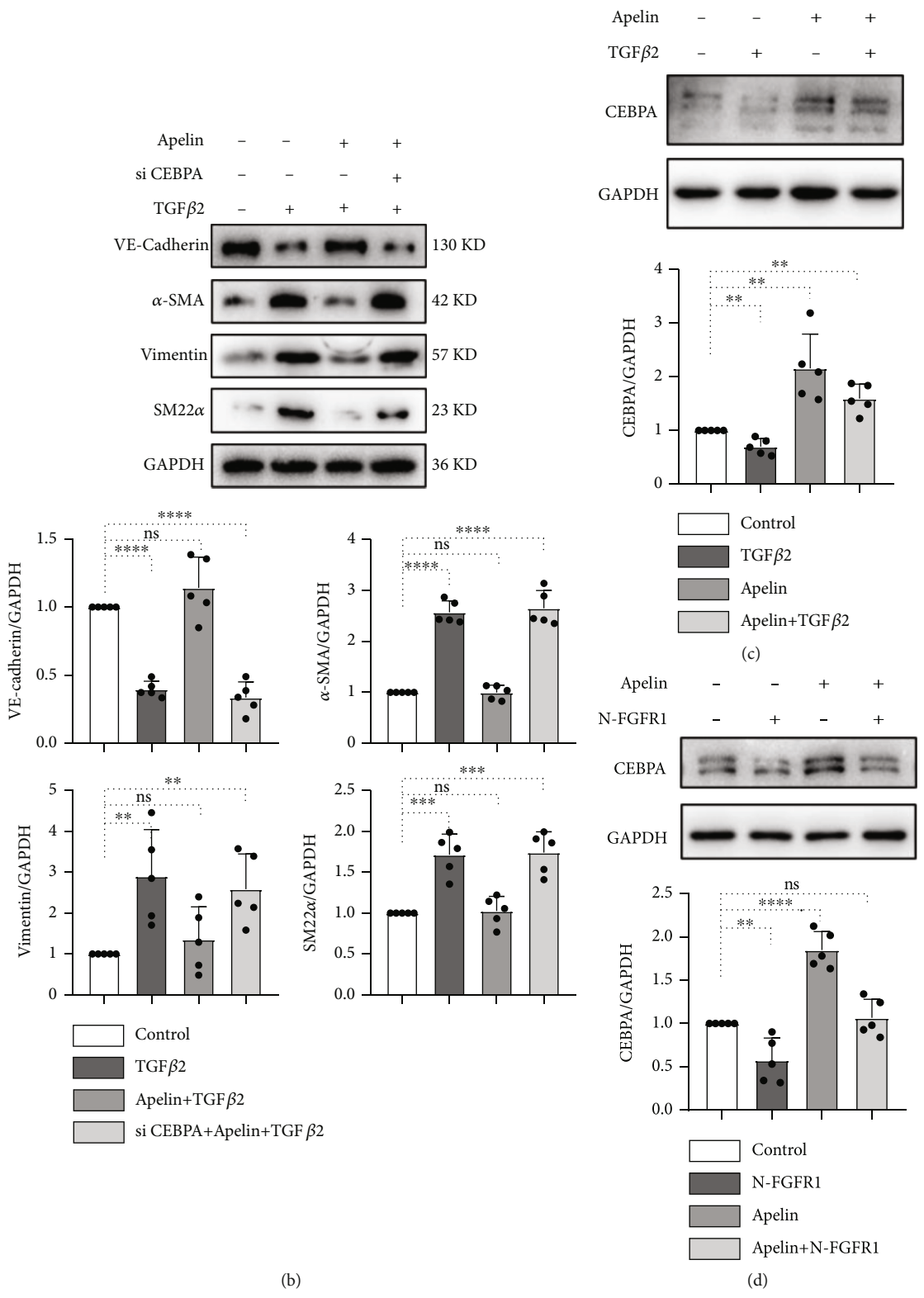

Figure 4: Continued.

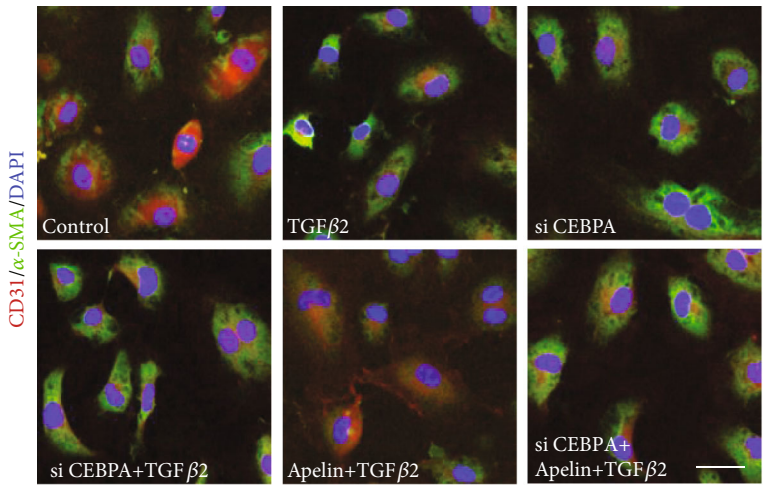

(e)

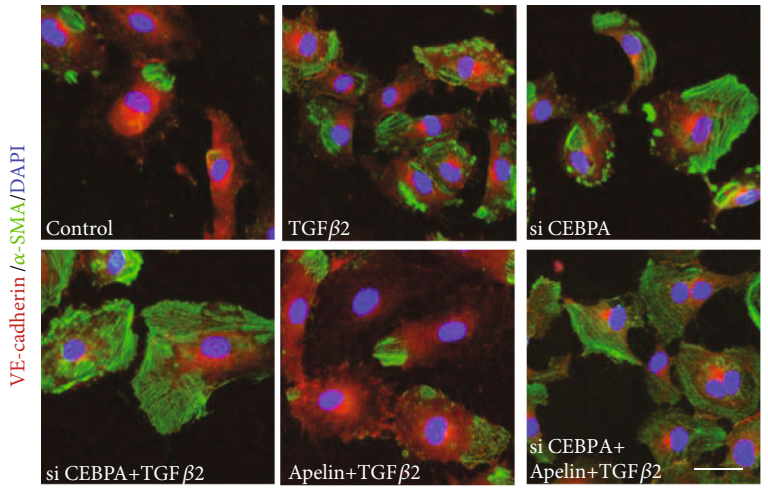

(f)

Figure 4: CEBPA knockdown promotes TGFβ-mediated EndMT. (a) HMVECs were transfected with or without CEBPA siRNA for 48 h in the presence or absence of TGFβ2, and the VE-cadherin, α-SMA, vimentin, and SM22α levels were analyzed by western blot. Densitometric analysis of the VE-cadherin/GADPH, α-SMA/GADPH, vimentin/GADPH, and SM22α/GADPH levels from each group ($n = 5$) was analyzed. (b) HMVECs were transfected with CEBPA siRNA for 48 h in the presence or absence of TGFβ2 and apelin, and the VE-cadherin, α-SMA, vimentin, and SM22α levels were analyzed by western blot. Densitometric analysis of the VE-cadherin/GADPH, α-SMA/GADPH, vimentin/GADPH, and SM22α/GADPH levels from each group ($n = 5$) was analyzed. (c) HMVECs were treated with TGFβ2 for 15 min or 48 h with or without preincubation with apelin for 2 h, and the CEBPA levels were analyzed by western blot. Densitometric analysis of the CEBPA/GADPH level from each group ($n = 5$) was analyzed. (d) HMVECs were treated with N-FGFR1 for 48 h or 15 min in the presence or absence of apelin, and the CEBPA levels was analyzed by western blot. Densitometric analysis of the CEBPA/GADPH level from each group ($n = 5$) was analyzed. Immunofluorescence analysis of CD31 (e) and α-SMA (f) coexpression in HUVECs following TGFβ2 or/and apelin or/and CEBPA siRNA treatment. For each slide, images of six different fields of view at ×200 magnification were evaluated. The scale bar is 50 μm in each panel.

III, SMAD-2, and SMAD-4 (supplementary Figure 1(a, b)). Apelin suppressed the level of miR-29 and promoted the level of miR-let-7 in both diabetes kidneys and HK2 cells (supplementary Figure 1(c, d)).

4. Discussion

In this study, we described the anti-EndMT and antifibrotic effects of apelin via the inhibition of TGFβ/Smad signaling. *In vitro*, we confirmed that apelin inhibited TGFβ-induced EndMT by increasing the abundance of FGFR1 in the endothelium, and conditioned medium from apelin-knockdown HUVECs mediated EMT activation in HK2 cells. Activation of TGFβ/Smad suppresses CEBPA expression, which mediates the initiation of EndMT in endothelial cells. *In vivo*, apelin ameliorated diabetes-induced renal fibrosis and glomerular damage, and the anti-EndMT effect of apelin was confirmed in endothelial cells of diabetic kidneys.

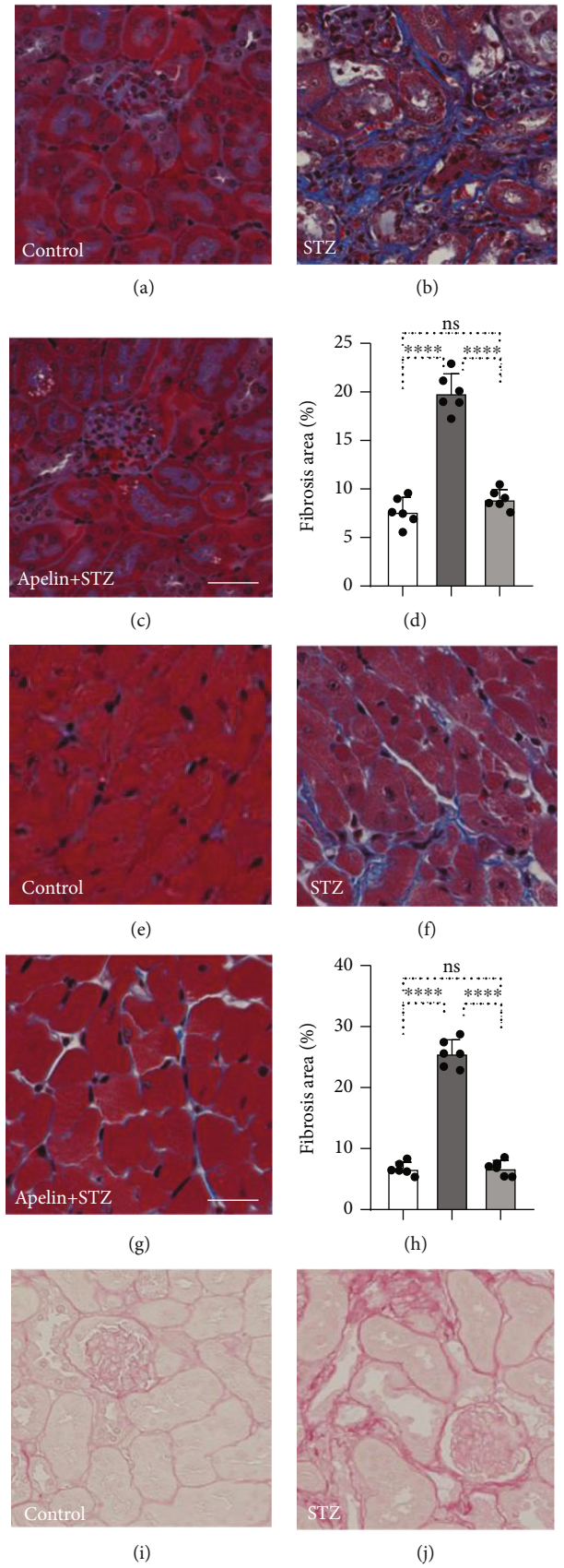

Figure 5: Continued.

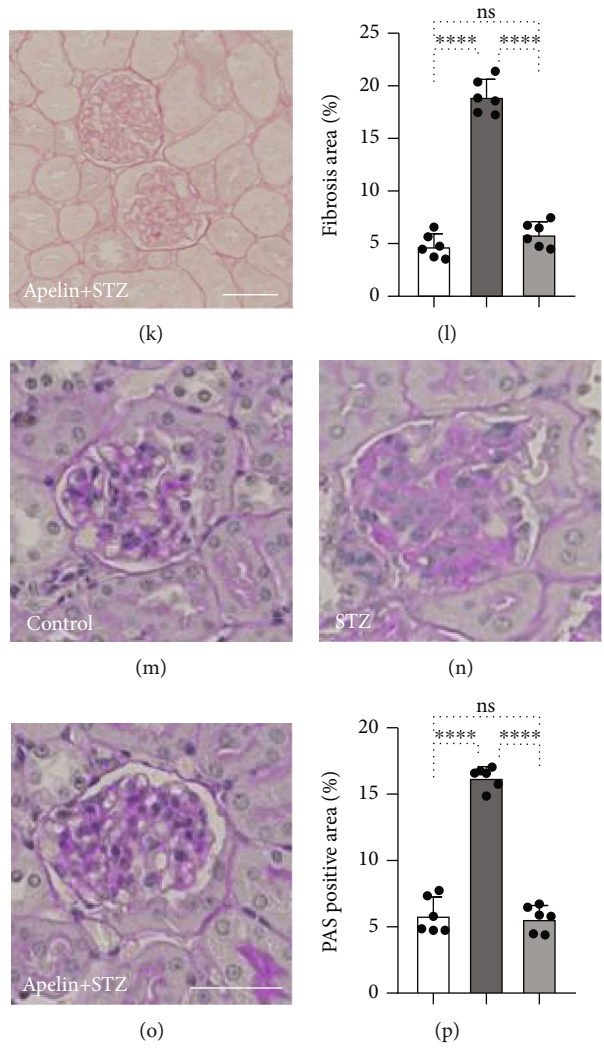

Figure 5: Apelin suppresses organ fibrosis and ameliorates diabetes-induced glomerular damage. Masson's trichrome staining (MTS) in the control (a), diabetic (b), and apelin-treated diabetic kidney (c). Scale bar: 40 μm. Quantification of relative fibrosis areas was calculated using the ImageJ software (d). MTS in the control (e), diabetic (f), and apelin-treated diabetic heart (g). Scale bar: 40 μm. Quantification of relative fibrosis areas was calculated using the ImageJ software (h). Sirius red staining in the control (i), diabetic (j), and apelin-treated diabetic kidney (k). Scale bar: 40 μm. Quantification of relative fibrosis areas was calculated using the ImageJ software (l). Periodic acid-Schiff (PAS) staining in the control (m), diabetic (n), and apelin-treated diabetic kidney (o). Scale bar: 60 μm. Quantification of the relative areas of glomeruli by the ImageJ software (p). For each section, images from six different fields of view at ×400 original magnification were obtained.

Fibroblast activation and parenchyma loss are the main characteristics of organ fibrosis [43, 44]. It has been reported that the apelin pathway is involved in the progression of pathological and physiological fibrosis, including kidney fibrosis, myocardial fibrosis, hepatic fibrosis, and pulmonary fibrosis [17, 43, 45]. Previous studies have reported that FGF/FGFR1 suppresses TGFβ-induced EndMT, which results in the proliferation of fibroblasts and deposition of the extracellular matrix [37, 46]. Although there is evidence of a microRNA-dependent correlation between apelin and FGF2/FGFR1 pathways in pulmonary artery endothelial cells [36], the molecular interactions between apelin and FGFR1 in TGFβ signaling are unclear. Our results showed that the close proximity between apelin and FGFR1 inhibited TGFβ/Smad signaling. The increased abundance of apelin inhibited TGFβ-induced EndMT by upregulating FGFR1 expression in the endothelium (Figure 1). FGFR1 deficiency reversed the anti-EndMT effect of apelin by targeting TGFβ/Smad signaling (Figures 1 and 2). A reverse effect was confirmed by the knockdown of apelin at the mRNA and protein levels (Figure 3).

Apelin inhibits TGFβ-dependent EMT in tubular epithelial cells to attenuate renal interstitial fibrosis [32]. Additionally, exogenous apelin has been shown to restore the EMT of podocytes, and decreased abundance of β5i enhanced the anti-EMT effect of apelin in podocytes in diabetic mice

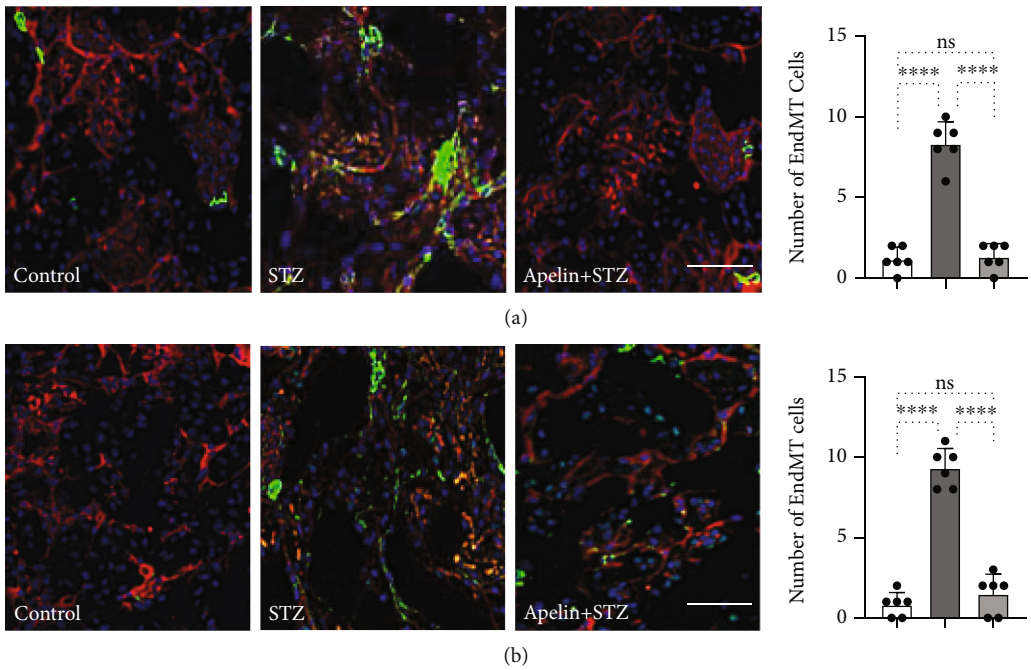

Figure 6: Apelin inhibits EndMT in diabetic kidneys. Immunofluorescence microscopy analysis of CD31/FSP1 (a) and CD31/α-SMA (b) in the kidney tissues from each group of mice. The scale bar is 40 μm in each panel. The CD31 and FSP1 double-positive cells, the CD31 and α-SMA double-positive cells, and the CD31 and vimentin double-positive cells were recognized as the cells undergoing EndMT. For each section, images from six different fields of view at ×400 original magnification were obtained. And the cells undergoing the EndMT were counted and quantified by the ImageJ software.

[33]. A recent study showed that the EndMT effect on peritubular capillaries could be induced by the EMT phenotype in proximal tubular cells through soluble factors [8]. Our results demonstrated that apelin deficiency in endothelial cells induced EMT in tubular epithelial cells, indicating that the EndMT phenotype of endothelial cells alters the phenotype of normal tubular epithelial cells (Figure 4).

Emerging evidence has shown that apelin exerts a protective effect against DN [23, 33, 47, 48]. Chen et al. and Day et al. reported that apelin acts as a suppressor of diabetes-induced inflammation, renal hypotrophy, and glomerular expansion in mice with type 1 diabetes [47, 48]. Liu et al. and Yin et al. confirmed the inhibitory effects of apelin on autophagy and EMT in podocytes of diabetic mice [23, 33]. Our study confirmed that apelin exhibited antifibrotic and anti-EndMT effects in endothelial cells in diabetic kidneys and hearts and remarkably ameliorated diabetes-induced glomerular damage (Figures 5 and 6). miR-29 and miR-let-7 were confirmed to contribute to pathological processes including kidney fibrosis [49]. Our results demonstrated that apelin suppressed the level of miR-29 and promoted the level of miR-let-7 (supplementary Figure 1).

CEBPA has been confirmed to be a Smad3-repressed target in TGFβ-induced EMT during tumorgenesis. In the presence of TGFβ treatment, nuclear Smad3 acts as a transcriptional repressor of CEBPA, and depletion of C/EBPα expression promotes the activation of EMT [41]. Similarly, we found that TGFβ-induced repression of CEBPA expression contributed to the initiation of EndMT. Apelin and the FGFR1 complex impaired EndMT by targeting the TGFβ/Smad/CEBPA axis (Figure 4).

5. Conclusion

In this study, we focused on the anti-EndMT and antifibrotic effects of apelin, which are generally thought to be important for kidney protection. First, the proximity of apelin and FGFR1 is critical for suppression of the TGFβ/Smad signaling pathway in the endothelium. Second, apelin inhibits TGFβ/Smad signaling and EndMT by regulating FGFR1 expression in endothelial cells. We found that the conditioned medium from apelin-knockdown HUVECs mediated the induction of EMT in HK2 cells. In addition, CEBPA knockdown promotes TGFβ-mediated EndMT. In vivo, apelin inhibited diabetes-induced EndMT. These data provide clear evidence of the anti-EndMT and antifibrotic effects of apelin via the inhibition of TGFβ/Smad signaling.

In conclusion, the results of this study revealed that the interaction of apelin and FGFR1 displayed renoprotective potential through suppression of the TGFβ/Smad/CEBPA-mediated EndMT/EMT pathway.

Data Availability

The data used to support the findings of this study are available from the corresponding author upon request.

Conflicts of Interest

The authors declare no conflict of interest.

Authors' Contributions

Rongfen Gao, Yumin Wu, Yang Qian, and Liangdong Chen contributed equally to this work.

Acknowledgments

This work was supported by the Improvement Project for Theranostic Ability with Difficulty Miscellaneous Disease.

Supplementary Materials

Materials and methods of supplementary figure: RNA extraction and qPCR. Total RNA was isolated using the miRNeasy kit (Qiagen) and quantified using a NanoDrop spectrophotometer (NanoDrop Technologies, DE, USA), according to the manufacturer's instructions. Complementary DNA (cDNA) was generated using a miScript II RT kit (Qiagen) and the HiSpec buffer method. miR expression was quantified using the miScript SYBR Green PCR Kit (Qiagen) with 3 ng of complementary DNA. Total RNA (50 ng of total RNA was reverse-transcribed using a TaqMan miRNA Reverse Transcription Kit with primers for miR-29, let-7, and Hs_RNU6-2_1 (Applied Biosystems). This was followed by an RT-PCR using a standard TaqMan microRNA assay protocol with TaqMan probes for these miRNAs. All experiments were performed in triplicates, and Hs_RNU6-2_1 was used as the internal control. Supplementary Figure 1: apelin inhibits EndMT not via angiogenesis protein and inflammatory protein in diabetic kidneys. (a) The collagen I, collagen III, fibronectin, Smad2, and Smad4 levels were analyzed by qPCR in the kidney tissues from each group of mice. (b) The VEGFR1 and VEGFR2 levels were analyzed by qPCR in the kidney tissues from each group of mice. (c) The levels of miR29 and miR-let-7s were analyzed by qPCR in the kidney tissues from each group of mice. (d) HK2 cells incubated with high glucose medium with or without the incubated with apelin for 48 h, and the levels of miR29 and miR-let-7s were analyzed by qPCR. *(Supplementary Materials)*

References

[1] M. V. Nastase, J. Zeng-Brouwers, M. Wygrecka, and L. Schaefer, "Targeting renal fibrosis: mechanisms and drug delivery systems," *Advanced Drug Delivery Reviews*, vol. 129, pp. 295–307, 2018.

[2] V. S. Roberts, P. J. Cowan, S. I. Alexander, S. C. Robson, and K. M. Dwyer, "The role of adenosine receptors A_{2A} and A_{2B} signaling in renal fibrosis," *Kidney International*, vol. 86, no. 4, pp. 685–692, 2014.

[3] M. Mack and M. Yanagita, "Origin of myofibroblasts and cellular events triggering fibrosis," *Kidney International*, vol. 87, no. 2, pp. 297–307, 2015.

[4] S. Lovisa, V. S. LeBleu, B. Tampe et al., "Epithelial-to-mesenchymal transition induces cell cycle arrest and parenchymal damage in renal fibrosis," *Nature Medicine*, vol. 21, no. 9, pp. 998–1009, 2015.

[5] M. T. Grande, B. Sánchez-Laorden, C. López-Blau et al., "Snail1-induced partial epithelial-to-mesenchymal transition drives renal fibrosis in mice and can be targeted to reverse established disease," *Nature Medicine*, vol. 21, no. 9, pp. 989–997, 2015.

[6] J. Li, S. Shi, S. P. Srivastava et al., "FGFR1 is critical for the anti-endothelial mesenchymal transition effect of N-acetyl-seryl-aspartyl-lysyl-proline via induction of the MAP4K4 pathway," *Cell Death & Disease*, vol. 8, no. 8, pp. e2965–e2965, 2017.

[7] A. S. Cruz-Solbes and K. Youker, "Epithelial to mesenchymal transition (EMT) and endothelial to mesenchymal transition (EndMT): role and implications in kidney fibrosis," *Results and Problems in Cell Differentiation*, vol. 60, pp. 345–372, 2017.

[8] J. Li, H. Liu, S. Takagi et al., "Renal protective effects of empagliflozin via inhibition of EMT and aberrant glycolysis in proximal tubules," *JCI Insight*, vol. 5, no. 6, 2020.

[9] S. P. Srivastava, J. Li, Y. Takagaki et al., "Endothelial SIRT3 regulates myofibroblast metabolic shifts in diabetic kidneys," *iScience*, vol. 24, no. 5, article 102390, 2021.

[10] L. Hong, X. Du, W. Li, Y. Mao, L. Sun, and X. Li, "EndMT: a promising and controversial field," *European Journal of Cell Biology*, vol. 97, no. 7, pp. 493–500, 2018.

[11] A. O. Jackson, J. Zhang, Z. Jiang, and K. Yin, "Endothelial-to-mesenchymal transition: a novel therapeutic target for cardiovascular diseases," *Trends in Cardiovascular Medicine*, vol. 27, no. 6, pp. 383–393, 2017.

[12] S. P. Srivastava, H. Zhou, O. Setia et al., "Loss of endothelial glucocorticoid receptor accelerates diabetic nephropathy," *Nature Communications*, vol. 12, no. 1, p. 2368, 2021.

[13] D. Medici, S. Potenta, and R. Kalluri, "Transforming growth factor-β2 promotes snail-mediated endothelial-mesenchymal transition through convergence of Smad-dependent and Smad-independent signalling," *The Biochemical Journal*, vol. 437, no. 3, pp. 515–520, 2011.

[14] E. Dejana, K. K. Hirschi, and M. Simons, "The molecular basis of endothelial cell plasticity," *Nature Communications*, vol. 8, no. 1, article 14361, 2017.

[15] A. Kitao, Y. Sato, S. Sawada-Kitamura et al., "Endothelial to mesenchymal transition via transforming growth factor-beta1/Smad activation is associated with portal venous stenosis in idiopathic portal hypertension," *The American Journal of Pathology*, vol. 175, no. 2, pp. 616–626, 2009.

[16] I. Castan-Laurell, C. Dray, C. Attané, T. Duparc, C. Knauf, and P. Valet, "Apelin, diabetes, and obesity," *Endocrine*, vol. 40, no. 1, pp. 1–9, 2011.

[17] P. Melgar-Lesmes, M. Perramon, and W. Jiménez, "Roles of the hepatic endocannabinoid and apelin systems in the pathogenesis of liver fibrosis," *Cell*, vol. 8, no. 11, article 1311, 2019.

[18] E. Y. Zhen, R. E. Higgs, and J. A. Gutierrez, "Pyroglutamyl apelin-13 identified as the major apelin isoform in human plasma," *Analytical Biochemistry*, vol. 442, no. 1, pp. 1–9, 2013.

[19] M. Cayabyab, S. Hinuma, M. Farzan et al., "Apelin, the natural ligand of the orphan seven-transmembrane receptor APJ, inhibits human immunodeficiency virus type 1 entry," *Journal of Virology*, vol. 74, no. 24, pp. 11972–11976, 2000.

[20] D. K. Lee, V. R. Saldivia, T. Nguyen, R. Cheng, S. R. George, and B. F. O'Dowd, "Modification of the terminal residue of

apelin-13 antagonizes its hypotensive action," *Endocrinology*, vol. 146, no. 1, pp. 231–236, 2005.

[21] I. Castan-Laurell, C. Dray, C. Knauf, O. Kunduzova, and P. Valet, "Apelin, a promising target for type 2 diabetes treatment?," *Trends in Endocrinology and Metabolism*, vol. 23, no. 5, pp. 234–241, 2012.

[22] M. Sawane, K. Kajiya, H. Kidoya, M. Takagi, F. Muramatsu, and N. Takakura, "Apelin inhibits diet-induced obesity by enhancing lymphatic and blood vessel integrity," *Diabetes*, vol. 62, no. 6, pp. 1970–1980, 2013.

[23] Y. Liu, J. Zhang, Y. Wang, and X. Zeng, "Apelin involved in progression of diabetic nephropathy by inhibiting autophagy in podocytes," *Cell Death & Disease*, vol. 8, no. 8, article e3006, 2017.

[24] J. Zhang, J. Yin, Y. Wang, B. Li, and X. Zeng, "Apelin impairs myogenic response to induce diabetic nephropathy in mice," *The FASEB Journal*, vol. 32, no. 8, pp. 4315–4327, 2018.

[25] S. Shi, S. P. Srivastava, M. Kanasaki et al., "Interactions of DPP-4 and integrin β1 influences endothelial-to-mesenchymal transition," *Kidney International*, vol. 88, no. 3, pp. 479–489, 2015.

[26] S. Shi, K. Kanasaki, and D. Koya, "Linagliptin but not sitagliptin inhibited transforming growth factor-β2-induced endothelial DPP-4 activity and the endothelial-mesenchymal transition," *Biochemical and Biophysical Research Communications*, vol. 471, no. 1, pp. 184–190, 2016.

[27] S. P. Srivastava, J. E. Goodwin, K. Kanasaki, and D. Koya, "Inhibition of angiotensin-converting enzyme ameliorates renal fibrosis by mitigating DPP-4 level and restoring antifibrotic microRNAs," *Genes*, vol. 11, no. 2, p. 211, 2020.

[28] A. A. Eddy, "Molecular basis of renal fibrosis," *Pediatric Nephrology*, vol. 15, no. 3-4, pp. 290–301, 2000.

[29] M. Iwano, D. Plieth, T. M. Danoff, C. Xue, H. Okada, and E. G. Neilson, "Evidence that fibroblasts derive from epithelium during tissue fibrosis," *The Journal of Clinical Investigation*, vol. 110, no. 3, pp. 341–350, 2002.

[30] D. Medici, E. M. Shore, V. Y. Lounev, F. S. Kaplan, R. Kalluri, and B. R. Olsen, "Conversion of vascular endothelial cells into multipotent stem-like cells," *Nature Medicine*, vol. 16, no. 12, pp. 1400–1406, 2010.

[31] E. M. Zeisberg, O. Tarnavski, M. Zeisberg et al., "Endothelial-to-mesenchymal transition contributes to cardiac fibrosis," *Nature Medicine*, vol. 13, no. 8, pp. 952–961, 2007.

[32] L.-Y. Wang, Z. L. Diao, D. L. Zhang et al., "The regulatory peptide apelin: a novel inhibitor of renal interstitial fibrosis," *Amino Acids*, vol. 46, no. 12, pp. 2693–2704, 2014.

[33] J. Yin, Y. Wang, J. Chang et al., "Apelin inhibited epithelial –mesenchymal transition of podocytes in diabetic mice through downregulating immunoproteasome subunits β5i," *Cell Death & Disease*, vol. 9, no. 10, p. 1031, 2018.

[34] I. S. Babina and N. C. Turner, "Advances and challenges in targeting FGFR signalling in cancer," *Nature Reviews Cancer*, vol. 17, no. 5, pp. 318–332, 2017.

[35] M. Katoh, "Therapeutics targeting FGF signaling network in human diseases," *Trends in Pharmacological Sciences*, vol. 37, no. 12, pp. 1081–1096, 2016.

[36] J. Kim, Y. Kang, Y. Kojima et al., "An endothelial apelin-FGF link mediated by miR-424 and miR-503 is disrupted in pulmonary arterial hypertension," *Nature Medicine*, vol. 19, no. 1, pp. 74–82, 2013.

[37] P. Y. Chen, L. Qin, G. Tellides, and M. Simons, "Fibroblast growth factor receptor 1 is a key inhibitor of TGFβ signaling in the endothelium," *Science Signaling*, vol. 7, no. 344, p. ra90, 2014.

[38] T. Nagai, M. Kanasaki, S. P. Srivastava et al., "N-acetyl-seryl-aspartyl-lysyl-proline inhibits diabetes-associated kidney fibrosis and endothelial-mesenchymal transition," *BioMed Research International*, vol. 2014, Article ID 696475, 12 pages, 2014.

[39] J. Li, H. Liu, S. P. Srivastava et al., "Endothelial FGFR1 (fibroblast growth factor receptor 1) deficiency contributes differential fibrogenic effects in kidney and heart of diabetic mice," *Hypertension*, vol. 76, no. 6, pp. 1935–1944, 2020.

[40] S. P. Srivastava, J. Li, M. Kitada et al., "SIRT3 deficiency leads to induction of abnormal glycolysis in diabetic kidney with fibrosis," *Cell Death & Disease*, vol. 9, no. 10, p. 997, 2018.

[41] A. R. Lourenço, M. G. Roukens, D. Seinstra et al., "C/EBPα is crucial determinant of epithelial maintenance by preventing epithelial-to-mesenchymal transition," *Nature Communications*, vol. 11, no. 1, p. 785, 2020.

[42] K. Miao, J. H. Lei, M. V. Valecha et al., "NOTCH1 activation compensates BRCA1 deficiency and promotes triple-negative breast cancer formation," *Nature Communications*, vol. 11, no. 1, article 3256, 2020.

[43] S. Huang, L. Chen, L. Lu, and L. Li, "The apelin-APJ axis: a novel potential therapeutic target for organ fibrosis," *Clinica Chimica Acta*, vol. 456, pp. 81–88, 2016.

[44] A. K. Ghosh, S. E. Quaggin, and D. E. Vaughan, "Molecular basis of organ fibrosis: potential therapeutic approaches," *Experimental Biology and Medicine (Maywood, N.J.)*, vol. 238, no. 5, pp. 461–481, 2013.

[45] Z. Z. Zhang, W. Wang, H. Y. Jin et al., "Apelin is a negative regulator of angiotensin II-mediated adverse myocardial remodeling and dysfunction," *Hypertension*, vol. 70, no. 6, pp. 1165–1175, 2017.

[46] P. Y. Chen, L. Qin, C. Barnes et al., "FGF regulates TGF-β signaling and endothelial-to-mesenchymal transition via control of let-7 miRNA expression," *Cell Reports*, vol. 2, no. 6, pp. 1684–1696, 2012.

[47] H. Chen, J. Li, L. Jiao et al., "Apelin inhibits the development of diabetic nephropathy by regulating histone acetylation in Akita mouse," *The Journal of Physiology*, vol. 592, no. 3, pp. 505–521, 2014.

[48] R. T. Day, R. C. Cavaglieri, and D. Feliers, "Apelin retards the progression of diabetic nephropathy," *American Journal of Physiology. Renal Physiology*, vol. 304, no. 6, pp. F788–F800, 2013.

[49] S. P. Srivastava, A. F. Hedayat, K. Kanasaki, and J. E. Goodwin, "microRNA crosstalk influences epithelial-to-mesenchymal, endothelial-to-mesenchymal, and macrophage-to-mesenchymal transitions in the kidney," *Frontiers in Pharmacology*, vol. 10, p. 904, 2019.